Clinical, pathological, and computed tomography morphological features of lung cancer with spread through air spaces

Xiuming Zhang[1#], Wei Qiao[1#], Jiannan Shen[2], Qianlai Jiang[1], Chunhan Pan[1], Yunnong Wang[1], Joanna Bidzińska[3], Feng Dai[4*], Lei Zhang[1*]

[1]Department of Radiology, Jiangsu Cancer Hospital & Jiangsu Institute of Cancer Research & The Affiliated Cancer Hospital of Nanjing Medical University (NMU), Nanjing, China; [2]Department of Thoracic Surgery, Jiangsu Cancer Hospital & Jiangsu Institute of Cancer Research & The Affiliated Cancer Hospital of Nanjing Medical University (NMU), Nanjing, China; [3]Second Department of Radiology, Medical University of Gdansk, Gdansk, Poland; [4]Department of Interventional Radiology, The Second Hospital of Nanjing, Nanjing University of Chinese Medicine, Nanjing, China

Contributions: (I) Conception and design: X Zhang, F Dai, L Zhang; (II) Administrative support: X Zhang, F Dai; (III) Provision of study materials or patients: J Shen; (IV) Collection and assembly of data: Q Jiang, C Pan, Y Wang; (V) Data analysis and interpretation: W Qiao; (VI) Manuscript writing: All authors; (VII) Final approval of manuscript: All authors.

[#]These authors contributed equally to this work as co-first authors.

[*]These authors contributed equally to this work as co-corresponding authors.

Correspondence to: Lei Zhang, MD. Department of Radiology, Jiangsu Cancer Hospital & Jiangsu Institute of Cancer Research, Baiziting, Xuanwu District, Nanjing 210000, China. Email: motozl163@163.com; Feng Dai, MD. Department of Interventional Radiology, The Second Hospital of Nanjing, Nanjing University of Chinese Medicine, Zhongfu Road, Nanjing 210003, China. Email: 13851560575@163.com.

Background: Spread through air spaces (STAS) is significantly associated with decreased overall survival (OS) and reduced recurrence-free survival. However, there are no reliable methods to confirm the presence of STAS before surgery. The sensitivity and specificity of the intraoperative frozen section diagnosis of STAS are not satisfactory. This study sought to determine the clinical, pathological, and computed tomography (CT) features of lung cancer with STAS before surgery to guide treatment decisions.

Methods: The data of 121 patients who were positive for STAS and 121 who were negative for STAS as confirmed by surgery and pathology were collected at Jiangsu Cancer Hospital from January 2020 to December 2022. The differences between the two groups in terms of the clinical, pathological, and CT characteristics were compared.

Results: STAS occurred not only in lung adenocarcinoma (LUAD) (106 of 121, 87.6%), but also in other pathological types of lung cancer (15 of 121, 12.4%). STAS was significantly correlated with pathological invasiveness [pathological differentiation, tumor, node, metastasis (TNM) staging, vascular invasion, and pleural invasion; all $P<0.05$]. STAS was most common in solid tumors (95 of 121, 78.51%). The receiver operating characteristic (ROC) curve showed that the optimal cut-off value for diagnosing STAS based on diameter is 1.55 cm with a sensitivity of 73.3% and a specificity of 47.9%. The percentage of solid components (PSC) is an independent influencing factor of lung cancer with STAS [odds ratio (OR) =111.27; $P<0.05$] with an optimal cut-off value of 63%, a sensitivity of 92.5%, and a specificity of 72.7%. In the part-solid nodules, the occurrence rate of STAS increased as the PSC increased. STAS was only observed in part-solid nodules with a PSC greater than 25%. Among the CT morphological features, lobulation was an independent influencing factor of lung cancer with STAS (OR =3.513; $P<0.05$), and persistent indistinct margin ground-glass opacity around the primary lesion of lung cancer (21 of 121, 17.36%) and satellite foci (9 of 121, 7.44%) strongly indicated the existence of STAS.

Conclusions: The clinical, pathological and CT features of STAS may guide clinicians to develop appropriate strategies and improve the survival rate of patients.

Keywords: Lung cancer; spread through air spaces (STAS); influencing factors; computed tomography (CT); ground-glass nodule

Introduction

In 2015, the World Health Organization defined spread through air spaces (STAS) as the "extension of tumor cells in the form of micropapillary cell clusters, solid cancer nests, or individual tumor cells from the edge of the primary tumor into the surrounding lung parenchyma through the air spaces" (1,2). STAS was formally introduced and recognized as a new pattern of invasion in lung adenocarcinoma (LUAD) (3). Extensive studies have shown that STAS is a morphological indicator of poor prognosis and a major risk factor for early lung cancer recurrence following limited resection because it is significantly associated with decreased overall survival (OS) and reduced recurrence-free survival (1-3). Previous studies have also attempted to detect STAS intraoperatively using frozen sections, but the sensitivity of predicting STAS through frozen sections is not high (4-6). Currently, STAS detection relies on the use of postoperative paraffin sections, which incurs a certain time lag and cannot be used to guide the clinical development of treatment strategies. For local treatments, including stereotactic radiotherapy and radiofrequency ablation, the identification of STAS could play a role in determining whether the ablation margin is sufficient (7). Thus, the ability to accurately predict STAS using preoperative imaging methods or before local treatment could contribute to the refinement of treatment plans. We present this article in accordance with the STARD reporting checklist (available at https://tlcr. amegroups.com/article/view/10.21037/tlcr-24-715/rc).

Highlight box

Key findings

- The identification of specific computed tomography (CT) features, particularly the percentage of solid components (PSC), and morphological characteristics, provides a valuable approach for predicting spread through air spaces (STAS) and guiding clinical treatment planning.

What is known, and what is new?

- Most previous studies reported that STAS was higher in lung cancer patients with solid nodules than it was in those with sub-solid nodules. This study further stratified part-solid nodules, and revealed that STAS was only observed in part-solid nodules with a solid component greater than 25%. The PSC is an independent influencing factor of lung cancer with STAS.
- Most previous studies reported that differences were existed between the STAS-positive and STAS-negative group in terms of the CT morphological features, such as lobulation and burrs. This study revealed that in addition to lobulation and burrs, persistent indistinct margin ground-glass opacity around the primary lesion of lung cancer and satellite foci also strongly indicate the existence of STAS.

What is the implication and what should change now?

- When performing localized segmental resection, this study showed that the margin should be at least greater than 1.55 cm to avoid local or distant recurrence caused by STAS.
- Caution should be exercised when considering segmental resection for part-solid nodules with a diameter of less than 2 cm and a PSC greater than 63% to avoid increasing the risk of local recurrence

Methods

General information

The study was conducted in accordance with the Declaration of Helsinki (as revised in 2013). This retrospective study was approved by the Ethics Committee of Nanjing Medical University (No. 2021-426), and the requirement for patient's informed consent was waived. A total of 154 patients with lung cancer with STAS, as confirmed by surgical pathology at Jiangsu Cancer Hospital from January 2020 to December 2022, were enrolled in the study. During the same period, 121 patients with lung cancer without STAS as confirmed by surgical pathology were randomly selected and included in the study as the control group. Patients who met any of the following criteria were excluded from the study: (I) had multiple nodules; (II) lacked preoperative computed tomography (CT) data; (III) had a history of previous tumors; and/or (IV) had undergone neoadjuvant chemotherapy, immunotherapy, or radiation therapy before surgery (*Figure 1*). All personal information of the patients was anonymized during the study.

Examination methods
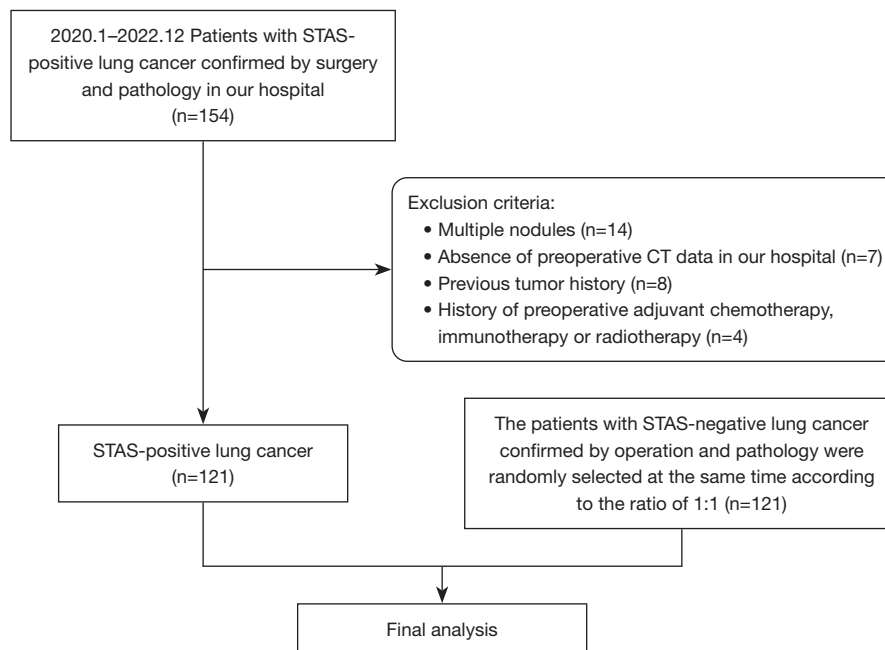
The LightSpeed volume CT (VCT) and Discovery 750HD

Figure 1 Flowchart showing patient inclusion and exclusion in the study. STAS, spread through air spaces; CT, computed tomography.

systems (GE Healthcare, Chicago, IL, USA) were used to conduct the CT examinations. The patients were positioned supine, and iohexol or ioversol (Jiangsu Hengrui Medicine, Lianyungang, China) was rapidly injected through the elbow vein using high-pressure injection at a rate of 1.0 mL/s and a dose of 1.5 mL/kg. Scanning was initiated approximately 30 seconds after the injection. The scanning range ran from the thoracic inlet to below the costophrenic angle. The tube current was set in a range of 200 to 280 mA, and the tube voltage was fixed at 120 kV. A preliminary helical volumetric scan was performed with a slice thickness of 0.625×64 mm, a matrix size of 512×512, and a pitch of 0.984. Next, image reconstruction was conducted with slice thicknesses of 1.25 and 5 mm, along with corresponding interslice intervals of 1.25 and 5 mm. An iterative algorithm with a 30% iteration factor was used to reconstruct the spectral images.

All tumors were staged according to the tumor-node-metastasis classification of the American Joint Committee on Cancer Staging Manual (ninth edition) (8).

Image analysis

The CT observation indicators included the lesion type (solid, part-solid, pure ground glass, or cystic), diameter, percentage of solid components (PSC), location (peripheral or central), lesion shape (spherical, quasi-spherical, or irregular), margin (burr, lobed, or ground-glass shadow with blurred boundary), internal features (air bronchogram, vacuole, or cavity), and peripheral features (satellite foci or pleural retraction). The PSC was defined as the longest diameter of the solid component in the lesion divided by the longest diameter of the lesion, multiplied by 100%. To determine the location, the center was defined as being completely within two-thirds of the lung. A ground-glass shadow with a blurred boundary was defined as a fuzzy shadow with a blurred boundary around the lesion (not at the distal end). Satellite foci were defined as nodules within 2 cm of the primary lesion.

The image analysis involved a double-blind assessment by two physicians with more than 10 years of experience in chest imaging diagnosis. Consensus findings were directly recorded, and any disagreements were resolved by discussion between the two physicians.

Statistical analysis

The data analysis was performed using the software SPSS 26.0 (IBM Corp., Armonk, NY, USA). The measurement data are presented as the mean ± standard deviation, and the count data are expressed as the quantity (proportion). The Kolmogorov-Smirnov test was employed to assess whether the measurable variables were normally distributed. For the

Table 1 Differences in clinical characteristics between the STAS-positive and STAS-negative groups

Clinical characteristics	STAS-positive group (N=121)	STAS-negative group (N=121)	Stat[†]	P value
Gender			3.251	0.07
Male	64 (52.89)	50 (41.32)		
Female	57 (47.11)	71 (58.68)		
Age (years)	62.01±10.00	59.59±10.16	1.896	0.06
History of smoking			0.872	0.35
Yes	109 (90.08)	113 (93.39)		
No	12 (9.92)	8 (6.61)		

Data are presented as n (%) or mean ± standard deviation. [†], In an independent samples *t*-test, the term "stat" refers to the t value. In a Mann-Whitney *U* test, "stat" refers to the Z value. For a chi-square test, "stat" refers to the Pearson value. STAS, spread through air spaces.

normally distributed variables, an independent sample *t*-test was used, and for the non-normally distributed variables, an analysis of variance and the Mann-Whitney *U* test were used. To compare differences in the CT features among all groups, the Chi-square test or Fisher's exact probability test was employed. The receiver operating characteristic (ROC) curve was employed to assess the diagnostic efficiency of the diameter and PSC. For factors exhibiting significant differences, a multivariate binary logistic regression analysis was conducted to determine the primary influencing factors. A P value <0.05 was considered statistically significant.

Results

Clinical features

The gender ratio was 64:57 in the STAS-positive group and 50:71 in the STAS-negative group. The median age was 64 years in the STAS-positive group and 60 years in the STAS-negative group. In the STAS-positive group, 90.08% (109/121) had a history of smoking. While in the STAS-negative group, 93.39% (113/121) had a history of smoking. The univariate analysis revealed no significant differences between the two groups in terms of gender, age, or history of smoking. A total of 121 lesions were observed in the STAS-positive group and 121 lesions were observed in the STAS-negative group (*Table 1*).

Pathological features

In the STAS-positive group, there were 106 cases of pathologically confirmed LUAD, including four cases of mucinous component, 10 cases of squamous cell carcinoma, four cases of neuroendocrine carcinoma, and one case of

adenocarcinoma with partial neuroendocrinization. Of these patients, 74.38% (90/121) showed low to medium pathological differentiation, and 64.46% (78/121) had tumor, node, metastasis (TNM) stage I. In terms of invasion, 28.10% (34/121) of these patients had vascular invasion, and 47.93% (58/121) had pleural invasion. In terms of TNM stage, the incidence rate of STAS exhibited a gradual increase in stages I, II, and III (58.21%, 81.25%, and 96.77%, respectively).

In the STAS-negative group, there were 108 cases of LUAD, 10 cases of squamous cell carcinoma, one case of adenocarcinoma with partial neuroendocrinization, one case of neuroendocrine cancer, and one case of adenosquamous cell carcinoma. The pathological differentiation of these cases was good, including high, high-middle, and middle differentiation, with a proportion of 77.69% (94/121), and only 22.31% (27/121) had middle and low differentiation. In terms of TNM stage, 93.39% (113/121) of these patients had stage I. In terms of invasion, 0.83% (1/121) of the patients had vascular invasion, and 26.62% (31/121) had pleural invasion.

The univariate analysis revealed that there were significant differences between the two groups in terms of the degree of pathological differentiation, TNM stage, vascular invasion, and pleural invasion (*Table 2*).

CT features

The univariate analysis revealed significant differences between the two groups in terms of the diameter, classification, PSC, burr, lobule, vacuole, ground-glass shadow with or without boundary ambiguity, satellite focus, and pleural traction (P<0.05). STAS was primarily detected

Table 2 Differences in pathological characteristics between the STAS-positive and STAS-negative groups

Pathological characteristics	STAS-positive group (N=121)	STAS-negative group (N=121)	Stat[†]	P value
Type of pathology			2.107	<0.001[a]
Adenocarcinoma	106 (87.60)	108 (89.26)		
Squamous cell cancer	10 (8.26)	10 (8.26)		
Neuroendocrine cancer	4 (3.31)	1(0.83)		
Other	1 (0.83)	2 (1.65)		
Degree of pathological differentiation			110.366	<0.001
Low differentiation	84 (69.42)	10 (8.26)		
Middle-low differentiation	6 (4.96)	17 (14.05)		
Middle differentiation	29 (23.97)	45 (37.20)		
High-middle-differentiation	2 (1.65)	39 (32.23)		
High differentiation	0 (0.00)	10 (8.26)		
TNM staging			33.442	<0.001
IA	69 (57.02)	105 (86.78)		
IB	9 (7.44)	8 (6.60)		
IIA	4 (3.31)	1 (0.83)		
IIB	9 (7.44)	3 (2.48)		
IIIA	25 (20.66)	3 (2.48)		
IIIB	5 (4.13)	1 (0.83)		
T			5.084	0.11[a]
T1	97 (80.17)	106 (87.60)		
T2	21 (17.36)	11 (9.09)		
T3	2 (1.65)	4 (3.31)		
T4	1 (0.82)	0 (0.00)		
N			32.979	<0.001
N0	78 (64.46)	114 (94.21)		
N1	12 (9.91)	3 (2.48)		
N2	31 (25.63)	4 (3.31)		
N3	0 (0.00)	0 (0.00)		
Vascular invasion			132.071	<0.001
No	87 (71.90)	120 (99.17)		
Yes	34 (28.10)	1 (0.83)		
Pleural invasion			12.956	<0.001
No	63 (52.07)	90 (74.38)		
Yes	58 (47.93)	31 (25.62)		

Data are presented as n (%). [†], In an independent samples *t*-test, the term "stat" refers to the t value. In a Mann-Whitney *U* test, "stat" refers to the Z value. For a chi-square test, "stat" refers to the Pearson value. [a], Fisher test. STAS, spread through air spaces; TNM, tumor, node, metastasis.
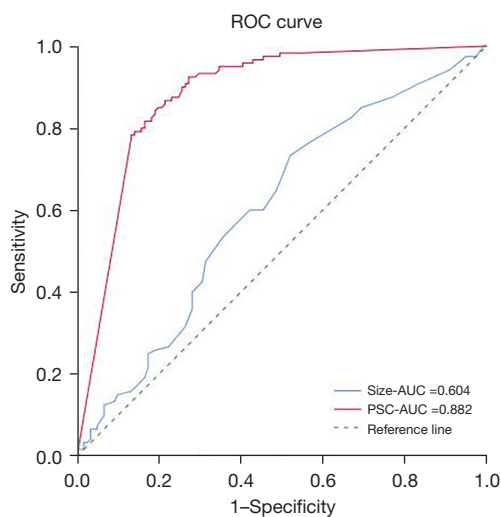
Figure 2 Receiver operating characteristic curve for assessing the diagnostic efficiency of the diameter and percentage of solid components. ROC, receiver operating characteristic; AUC, area under the curve; PSC, percentage of solid components.

in solid nodules (78.51%, 95/121). The optimal cut-off value of the diameter was 1.55 cm with a sensitivity of 73.3% and a specificity of 47.9% (*Figure 2*). The area under the curve for diagnosing STAS positivity in PSC was 0.882. The optimal cut-off value of PSC was 63% with a sensitivity of 92.5% and a specificity of 72.7% (*Figure 2*). Some solid nodules were stratified based on the PSC. STAS was only observed in nodules with a PSC greater than 25%, and the proportion of STAS increased as the solid components increased. The proportions of ground-glass shadows with blurred boundaries (*Figure 3*) and satellite foci (*Figure 4*) were 17.36% and 7.44%, respectively, and these were only observed in the STAS-positive lung cancer patients (*Table 3*).

Multivariate logistic regression

The multivariate logistic regression revealed that lobulation [odds ratio (OR) =3.513; P<0.001] and the PSC (OR =111.269; P<0.001) were independent influencing factors of
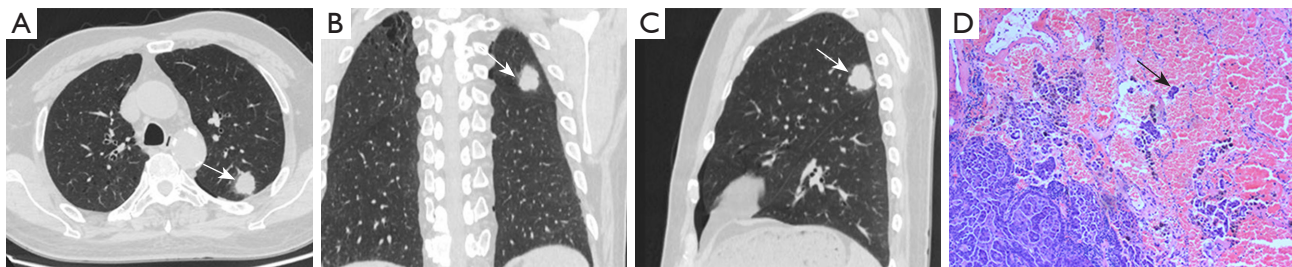

Figure 3 CT and pathological images of a 68-year-old man with lung cancer. (A-C) CT images showing a nodule in the left upper lung with lobulation and spiculation at the edges. Ground-glass opacity with a blurred border was observed around the nodule (non-distal) (white arrow). (D) Surgical pathology confirmed a poorly differentiated neuroendocrine carcinoma with STAS (black arrow). HE stain, 200×. CT, computed tomography; STAS, spread through air spaces; HE, hematoxylin and eosin.
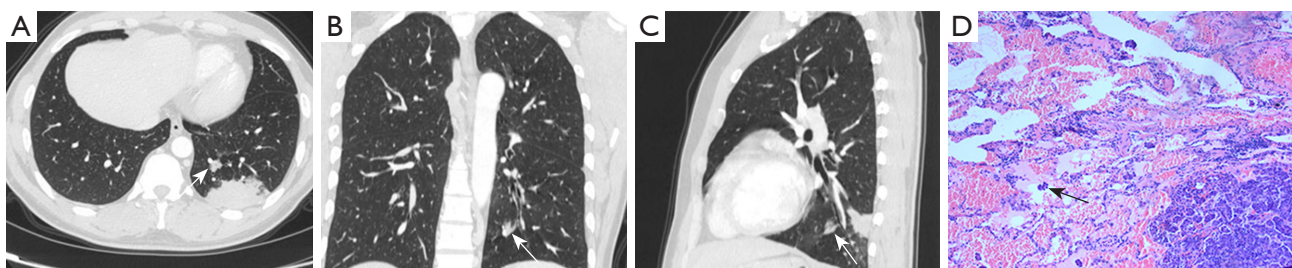

Figure 4 CT and pathological images of a 39-year-old man with lung cancer. (A-C) CT images showing a mass in the left lower lung. A mixed ground-glass nodule was identified 1.5 cm away from the mass (white arrow). (D) Surgical pathology confirmed that the mass was a peripheral nodular lung adenocarcinoma (papillary type 50%, acinous type 30%, micropapillary type 20%) with STAS (black arrow). HE stain, 200×. CT, computed tomography; STAS, spread through air spaces; HE, hematoxylin and eosin.

Table 3 Differences in CT characteristics between the STAS-positive and STAS-negative group

CT sign	STAS-positive group (N=121)	STAS-negative group (N=121)	Stat[†]	P value
Diameter (cm)	2.2736±1.1251	1.93±0.99	2.524	0.01
Categories				<0.001[a]
Solid	95 (78.51)	35 (28.93)		
Part-solid	22 (18.19)	48 (39.67)		
Pure ground glass	2 (1.65)	36 (29.75)		
Cystic	2 (1.65)	2 (1.65)		
PSC	0.92±0.18	0.37±0.38	10.823	<0.001*
Location			1.769	0.18
Central	50 (41.32)	40 (33.06)		
Periphery	71 (58.68)	81 (66.94)		
Burr			12.236	<0.001
No	77 (63.63)	101 (83.47)		
Yes	44 (36.37)	20 (16.53)		
Lobed			41.393	<0.001
No	33 (27.27)	83 (68.60)		
Yes	88 (72.73)	38 (31.40)		
Shape			1.669	0.20
Spherical or quasi spherical	96 (79.34)	80 (68.33)		
Irregular	25 (20.66)	41 (31.67)		
Vacuole			10.683	0.001
No	118 (97.52)	104 (86.00)		
Yes	3 (2.48)	17 (14.00)		
Cavity			3.483	0.054
No	110 (90.91)	117 (96.69)		
Yes	11 (9.09)	4 (3.31)		
Ground-glass shadows with blurred boundary			22.995	<0.001
No	100 (82.64)	121 (100.00)		
Yes	21 (17.36)	0 (0.00)		
Air bronchogram			0.162	0.69
No	79 (65.29)	76 (62.81)		
Yes	42 (34.71)	45 (37.19)		
Satellite foci				0.003
No	112 (92.56)	121 (100.00)		
Yes	9 (7.44)	0 (0.00)		
Pleural retraction			111.958	0.001
No	32 (26.45)	58 (47.93)		
Yes	89 (73.55)	63 (52.07)		

Data are presented as n (%) or mean ± standard deviation. [†], In an independent samples *t*-test, the term "stat" refers to the t value. In a Mann-Whitney *U* test, "stat" refers to the Z value. For a chi-square test, "stat" refers to the Pearson value. [a], Fisher test; *, the homogeneity test of variance and the Mann-Whitney *U* test was employed if the positive distribution did not conform to normal distribution. CT, computed tomography; STAS, spread through air spaces; PSC, percentage of solid components.

Table 4 Results of the multivariate logistic regression analysis

Parameter	P value	Exp(B)	95% confidence interval for Exp(B)
Lobed	0.002	3.513	1.590–7.761
PSC	<0.001	111.269	15.340–807.092
Constant	<0.001	0.033	–

PSC, percentage of solid components.

lung cancer with STAS (*Table 4*).

Discussion

Correlation of STAS with demographical and pathological characteristics

In this study, no significant correlation was observed between STAS and age, gender, and smoking history, and these results were consistent with those of most previous studies (1,9,10). Although no significant association was observed between STAS and pathological type (P>0.05), STAS was most common in LUAD (106/121). Most previous studies on STAS have primarily concentrated on LUAD (1,3,5,9,10); however, this study showed that STAS is not a unique pathological phenomenon of LUAD. STAS was also identified in squamous cell carcinoma (10/121), neurosecretory carcinoma (4/121), and other rare lung cancer types (1/121). In this study, STAS was found to be significantly correlated with the degree of pathological differentiation, vascular invasion, and pleural invasion (P<0.05). The proportion of middle-to-low and low differentiation in the STAS-positive group was 74.38%, which is consistent with the rate reported by Toyokawa *et al.* (11). The degree of pathological differentiation, vascular invasion, and pleural invasion were identified as factors correlated with pathological invasion and were predictive of a low survival rate. Thus, it was speculated that STAS could be another crucial or alternative factor in lung cancer aggressiveness. In this study, a significant correlation was also observed between STAS and the pathological TNM stage, and the incidence of STAS gradually increased as the TNM stage increased. Notably, STAS exhibited a relatively high positive rate (58.21%), even in stage I. In a study by Toyokawa *et al.* (12), among 276 cases of stage I LUAD, the positive rate of STAS was 55.4%, which is consistent with the results of this study. Thus, STAS should be considered when selecting a surgical approach for the

limited resection of stage I lung cancer.

Correlation between STAS and CT signs

Our study examined the correlation between STAS and CT signs. Statistically significant differences were observed between the STAS-positive group and the STAS-negative group in terms of the lesion diameter, classification, PSC, burrs, lobules, vacuoles, ground-glass shadows with blurred boundaries, satellite foci, and pleural traction (P<0.05). Conversely, no significant differences were observed in terms of the location, shape, voids, and air bronchogram (P>0.05). PSC and leaf lobulation were identified as independent factors in the multivariate regression analysis. This study revealed that the tumor diameter of the STAS-positive group was greater than that of the STAS-negative group, and this difference was statistically significant (P<0.05). The optimal cut-off value of the diameter was 1.55 cm with a sensitivity of 73.3% and a specificity of 47.9%. Several previous studies have shown that tumor diameter influences the incidence of STAS. Wang *et al.* (13) reported that tumors larger than 2 cm exhibited a higher proportion of STAS. According to the "Chinese Medical Association of Lung Cancer Diagnosis and Treatment 2023 Edition", when performing localized segmental resection for early lung cancer, the surgical margin should be greater than the maximum diameter of the lesion. To avoid local or distant recurrence caused by STAS, the margin should be at least greater than 1.55 cm (14).

Most studies have reported that the incidence of STAS is higher in lung cancer patients with solid nodules as shown on CT than in lung cancer patients with subsolid nodules (3,4). However, significant differences in nodule classification between the two groups have been identified. In this study, 78.5% of the STAS-positive group had solid nodules, which is consistent with previous studies (3,4). In recent years, the PSC has become a hot topic in lung cancer imaging studies and is an independent correlation factor for the recurrence and prognosis of early lung cancer (15,16). Notably, in this study, the PSC was more effective in predicting STAS than the tumor diameter. The PSC was easily obtained on CT, and had an optimal cut-off value of 63% with a sensitivity and specificity of 92.5% and 72.7%, respectively. This information could guide the reasonable treatment of lung cancer. Currently, it is controversial (17) whether pulmonary segmental resection is appropriate for pulmonary nodules located in the peripheral 1/2 area of lung, with a long diameter less than 2 cm, and a solid

component ratio greater than 0.5. Based on the findings of this study, it was concluded that caution should be exercised when considering segmental resection for part-solid nodules with a diameter of less than 2 cm and a PSC greater than 63% to avoid increasing the risk of local recurrence.

In this study, the part-solid nodules were further stratified, and the results showed that the positive rate of STAS increased as the PSC increased. Notably, STAS was only observed in part-solid nodules with a solid component greater than 25%. "China's National Expert Consensus on Thoracic Surgery for Lung Nodules (less than 2 cm) Wedge Resection 2023" recommends wedge resection for subsolid nodules with diameters less than 2 cm and PSC <0.25 (Class I recommendation). Importantly, the results of this study are consistent with this recommendation (18). Statistically significant differences were observed between the STAS-positive and STAS-negative groups in the lesions in terms of the burrs, lobulation, cavitation, ground-glass shadows with blurred boundaries, satellite foci, and pleural traction. Toyokawa *et al.* (10) also reported a correlation between STAS-positive and pleural depression, lobulation, burrs, and other signs. Tumors with malignant tendencies often display the imaging features of burrs, lobulation, and pleural stretch, and these features are associated with tumor invasiveness and poor prognosis.

Ground-glass nodules with blurred edges often indicate inflammation and bleeding, and ground-glass shadows with blurred boundaries may also appear around infiltrating mucinous adenocarcinoma, which is pathologically attributed to mucin filling the alveolar cavity, effusive macrophages, and tumor cells (19,20). The incidence of STAS in infiltrating mucinous adenocarcinoma is 50–70% (21). Ground-glass shadows with blurred boundaries were also detected at the tumor edge in the STAS-positive group. This study only included cases with blurred boundary glass shadows at the non-distal end of the lesion to differentiate obstructive pneumonia complicated by the tumor.

Blurred boundary glass shadows were only observed in 21 cases in the STAS-positive group, and no such shadows were observed in the STAS-negative group. The difference between the two groups was statistically significant. Thus, the persistence of ambiguous glass grinding at the tumor edge (non-distal) appears to be significantly correlated with STAS in lung cancer.

Warth *et al.* (22) discovered that peritumoral edema or bleeding provide a potential energy supply for STAS. Satellite foci are characteristic indicators of pulmonary tuberculosis, especially when accompanied by tree-bud signs, and have a predictive value of up to 90% for benign nodules (23). However, satellite foci are not unique to tuberculous spheres, and may also indicate peripheral lung cancer. Qi *et al.* (24) reported an incidence rate of approximately 5.36% for satellite foci in lung cancer. In this study, the incidence of satellite foci in the STAS-positive group reached 7.43% (9/121), and the CT scans revealed solid or ground-glass plaques or nodules within 2 cm of the primary lesion. Conversely, no such signs were observed in the STAS-negative group, and this difference achieved statistical significance, indicating a strong correlation between satellite foci and lung cancer-associated STAS.

The pathological basis of the formation of satellite foci in STAS is that changes in the internal and external environment of lung cancer result in the escape of tumor cells from the primary lesion, enabling them to migrate freely into the surrounding alveolar cavity in the form of micropapillary clusters or solid nests. This process reduces the gas content in the alveolar space. However, Uruga *et al.* (9) performed a semi-quantitative assessment of STAS, revealing that a significant proportion of STAS contained ≥5 single tumor cells or colonies, which were challenging to visualize on macro CT, resulting in a low detection rate on CT. It is hoped that the image detection method of STAS can be improved in the future. Anyway, persistent ground-glass shadows with blurred boundaries and satellite lesions around lung cancer are highly indicative of STAS. Lobectomy is the recommended surgical approach for these patients. The scope of surgery should be expanded if limited resection is considered for patients in whom lobectomy is not feasible because of various factors.

This study had some limitations. First, the study is retrospective, relying on data from a single institution These aspects increase the risk of bias in both inspection and observation. Second, our study has revealed that STAS is present not only in LUAD but also in other types of lung cancer. Nevertheless, owing to the limited number of cases, additional statistical analysis cannot be substantiated. In the future, we intend to investigate the association between STAS and other types of lung cancer. Third, recognizing tumor imaging signs through macroscopic observation is inherently subjective. STAS, often a microscopic histological characteristic, falls significantly below the spatial resolution offered by modern CT scans, thereby obscuring numerous subtle image details. Radiomics, however, offers a solution by enabling comprehensive analysis of CT images. This technology swiftly extracts quantitative internal features and converts them into minable big data, thereby facilitating the

extraction of valuable biological information from within the dataset. Fourth, we did not evaluate the relationship between STAS and molecular genetics, such as EGFR or PD-1, although we are committed to studying the imaging features of STAS.

Conclusions

STAS was not only observed in LUAD, but also in other histological types of lung cancer, and was significantly correlated with pathological invasiveness. STAS was primarily found in solid nodules, and the optimal cut-off value for diagnosing STAS was a diameter of 1.55 cm. The PSC was an independent factor of lung cancer with STAS, with an optimal cut-off value of 63%. In the part-solid nodules, the incidence of STAS increased as the solid components increased, and STAS only appeared in part-solid nodules with a PSC greater than 25%. In the CT morphological features, lobulation was an independent factor of lung cancer with STAS. Despite the relatively low proportion of persistent ground-glass shadows and satellite foci with blurred boundaries, both were strong indicators of STAS positivity. An analysis of these image characteristics could offer valuable insights into the possible existence of STAS, guiding the clinical formulation of optimal treatment strategies and enhancing the survival rates of patients.

Acknowledgments

Footnote

Reporting Checklist: The authors have completed the STARD reporting checklist. Available at https://tlcr.amegroups.com/article/view/10.21037/tlcr-24-715/rc

Data Sharing Statement: Available at https://tlcr.amegroups.com/article/view/10.21037/tlcr-24-715/dss

Peer Review File: Available at https://tlcr.amegroups.com/article/view/10.21037/tlcr-24-715/prf

Conflicts of Interest: All authors have completed the ICMJE uniform disclosure form (available at https://tlcr.amegroups.com/article/view/10.21037/tlcr-24-715/coif). The authors have no conflicts of interest to declare.

Ethical Statement: The authors are accountable for all aspects of the work in ensuring that questions related to the accuracy or integrity of any part of the work are appropriately investigated and resolved. The study was conducted in accordance with the Declaration of Helsinki (as revised in 2013). This retrospective study was approved by the Ethics Committee of Nanjing Medical University (No. 2021-426), and the requirement for patient's informed consent was waived.

References

1. Kadota K, Nitadori JI, Sima CS, et al. Tumor Spread through Air Spaces is an Important Pattern of Invasion and Impacts the Frequency and Location of Recurrences after Limited Resection for Small Stage I Lung Adenocarcinomas. J Thorac Oncol 2015;10:806-14.
2. Travis WD, Eisele M, Nishimura KK, et al. The International Association for the Study of Lung Cancer (IASLC) Staging Project for Lung Cancer: Recommendation to Introduce Spread Through Air Spaces as a Histologic Descriptor in the Ninth Edition of the TNM Classification of Lung Cancer. Analysis of 4061 Pathologic Stage I NSCLC. J Thorac Oncol 2024;19:1028-51.
3. Shiono S, Yanagawa N. Spread through air spaces is a predictive factor of recurrence and a prognostic factor in stage I lung adenocarcinoma. Interact Cardiovasc Thorac Surg 2016;23:567-72.
4. Walts AE, Marchevsky AM. Current Evidence Does Not Warrant Frozen Section Evaluation for the Presence of Tumor Spread Through Alveolar Spaces. Arch Pathol Lab Med 2018;142:59-63.
5. de Margerie-Mellon C, Onken A, Heidinger BH, et al. CT Manifestations of Tumor Spread Through Airspaces in Pulmonary Adenocarcinomas Presenting as Subsolid Nodules. J Thorac Imaging 2018;33:402-8.
6. Xu Y, Chen DL, Xu XJ, et al. Impact of tumor spread

through air spaces on surgical decision-making and accuracy of identifying spread through air spaces on frozen sections: A systematic review and meta-analysis. Chin J Clin Thorac Cardiovasc Surg 2024;31:900-9.

7. Loganadane G, Martinetti F, Mercier O, et al. Stereotactic ablative radiotherapy for early stage non-small cell lung cancer: A critical literature review of predictive factors of relapse. Cancer Treat Rev 2016;50:240-6.

8. Rami-Porta R, Nishimura KK, Giroux DJ, et al. The International Association for the Study of Lung Cancer Lung Cancer Staging Project: Proposals for Revision of the TNM Stage Groups in the Forthcoming (Ninth) Edition of the TNM Classification for Lung Cancer. J Thorac Oncol 2024;19:1007-27.

9. Uruga H, Fujii T, Fujimori S, et al. Semiquantitative Assessment of Tumor Spread through Air Spaces (STAS) in Early-Stage Lung Adenocarcinomas. J Thorac Oncol 2017;12:1046-51.

10. Toyokawa G, Yamada Y, Tagawa T, et al. Computed tomography features of resected lung adenocarcinomas with spread through air spaces. J Thorac Cardiovasc Surg 2018;156:1670-1676.e4.

11. Toyokawa G, Yamada Y, Tagawa T, et al. Significance of spread through air spaces in early-stage lung adenocarcinomas undergoing limited resection. Thorac Cancer 2018;9:1255-61.

12. Toyokawa G, Yamada Y, Tagawa T, et al. Significance of Spread Through Air Spaces in Resected Pathological Stage I Lung Adenocarcinoma. Ann Thorac Surg 2018;105:1655-63.

13. Wang Y, Lyu D, Zhang D, et al. Nomogram based on clinical characteristics and radiological features for the preoperative prediction of spread through air spaces in patients with clinical stage IA non-small cell lung cancer: a multicenter study. Diagn Interv Radiol 2023;29:771-85.

14. Park S, Lee SM, Choe J, et al. Differences in the prognostic implication of ground-glass opacity on CT according to pathological nodal status in lung cancers treated with lobectomy or pneumonectomy. Eur Radiol 2022;32:4405-13.

15. Zhang Z, Zhou L, Min X, et al. Long-term follow-up of persistent pulmonary subsolid nodules: Natural course of pure, heterogeneous, and real part-solid ground-glass nodules. Thorac Cancer 2023;14:1059-70.

16. Gao Z, Liu S, Xiao H, et al. Development and validation of a clinical decision tool for preoperative micropapillary and solid pattern lung adenocarcinoma of CT≤2 cm. Int J Surg 2024. [Epub ahead of print]. doi: 10.1097/JS9.0000000000001832.

17. Saji H, Okada M, Tsuboi M, et al. Segmentectomy versus lobectomy in small-sized peripheral non-small-cell lung cancer (JCOG0802/WJOG4607L): a multicentre, open-label, phase 3, randomised, controlled, non-inferiority trial. Lancet 2022;399:1607-17.

18. Tong X, Xu S, Wang S, et al. Clinical experience of the treatment of solitary pulmonary nodules with Da Vinci surgical system. Zhongguo Fei Ai Za Zhi 2014;17:541-4.

19. Miyata N, Endo M, Nakajima T, et al. High-resolution computed tomography findings of early mucinous adenocarcinomas and their pathologic characteristics in 22 surgically resected cases. Eur J Radiol 2015;84:993-7.

20. Kim H, Park CM, Koh JM, et al. Pulmonary subsolid nodules: what radiologists need to know about the imaging features and management strategy. Diagn Interv Radiol 2014;20:47-57.

21. Watanabe H, Saito H, Yokose T, et al. Relation between thin-section computed tomography and clinical findings of mucinous adenocarcinoma. Ann Thorac Surg 2015;99:975-81.

22. Warth A, Muley T, Kossakowski CA, et al. Prognostic Impact of Intra-alveolar Tumor Spread in Pulmonary Adenocarcinoma. Am J Surg Pathol 2015;39:793-801.

23. Jacob M, Romano J, Ara Jo D, et al. Predicting lung nodules malignancy. Pulmonology 2022;28:454-60.

24. Qi L, Xue K, Cai Y, et al. Predictors of CT Morphologic Features to Identify Spread Through Air Spaces Preoperatively in Small-Sized Lung Adenocarcinoma. Front Oncol 2020;10:548430.